#1A - Dupl

PUB-74-119-E
E-0001

#1A
PRL

MEASUREMENT OF RATES FOR MUONLESS DEEP INELASTIC NEUTRINO AND ANTINEUTRINO INTERACTIONS*

B. Aubert[⊥], A. Benvenuti, D. Cline, W. T. Ford, R. Imlay

T. Y. Ling, A. K. Mann, F. Messing, J. Pilcher**,

D. D. Reeder, C. Rubbia, R. Stefanski and L. Sulak

Department of Physics
Harvard University
Cambridge, Massachusetts 02138

Department of Physics
University of Pennsylvania
Philadelphia, Pennsylvania 19174

Department of Physics
University of Wisconsin
Madison, Wisconsin 53706

National Accelerator Laboratory
Batavia, Illinois 60510

ABSTRACT

Relative rates for deep inelastic neutrino and antineutrino scattering without a final state muon have been measured. For neutrinos the result is $R^{\nu} = \sigma(\nu_\mu + \text{nucleon} \to \nu_\mu + \text{hadrons})/\sigma(\nu_\mu + \text{nucleon} \to \mu^- + \text{hadrons}) = 0.11 \pm 0.05$. The corresponding ratio for antineutrinos is $R^{\bar{\nu}} = 0.32 \pm 0.09$.

We have reported previously[1,2] the observation of deep inelastic neutrino and antineutrino interactions in which no muon appeared in the final state. In those experiments a value of R, the ratio of the number of events without to the number of events with a muon, was obtained utilizing mixed neutrino-antineutrino beams with different admixtures. The subject of this paper is the determination of the individual ratios R^{ν} and $R^{\bar{\nu}}$, appropriate to incident beams of pure neutrinos and pure antineutrinos, respectively.

The experiments were carried out at the National Accelerator Laboratory, where collisions of 300 GeV protons with a target produced secondary hadrons which decay to provide the various neutrino-antineutrino beams. Data for the present study consist of three samples of neutrino- and antineutrino-induced inelastic interactions obtained with the detector, and analyzed by the methods, described in reference 2. Each sample is characterized by a different value of α, where α measures the admixture of interacting neutrinos and antineutrinos observed in those events with a muon in the final state; α is the measured ratio of events with negative muons to all events with muons, corrected for the different experimental detection efficiencies for negative and positive muons. Each sample was analyzed to extract the value of R, which is related to R^{ν} and $R^{\bar{\nu}}$ by,

$$R = \alpha R^{\nu} + (1-\alpha)\ R^{\bar{\nu}}. \qquad (1)$$

For a pure neutrino or antineutrino beam, eq. (1) reduces to $R = R^{\nu}$ or $R = R^{\bar{\nu}}$, respectively.

One of the data samples is essentially the same as that described earlier.[2] It was obtained with a mixed neutrino-antineutrino beam which was made by focusing negative pions and kaons with a magnetic horn to enrich the antineutrino component. Because the magnetic field of the horn was pulsed on for a period shorter than the duration of the beam spill and a little out of phase with it, the degree of focusing and hence the mixing parameter varied with time during each accelerator pulse. The beam spill as a function of time is shown in Fig. 1a. The variation of α with time is shown in Fig. 1b. Dividing the data into two subsamples, one with a large average value of α and one with a small average value of α, we obtain two relations of the form of equation (1) which can be solved for R^{ν} and $R^{\bar{\nu}}$.

The other two data samples were acquired using essentially pure beams of neutrinos and antineutrinos ($\alpha \approx 0.98$ or $\alpha \approx 0.12$). These beams were produced by sign selection of the charge of the secondary hadrons.[3]

The analysis of the resulting four data sets is summarized in Table I. As described in reference 2, three identifiers of muons were used to provide different muon detection efficiencies ϵ_{μ}, and different probabilities ϵ_p for the penetration by hadrons of the hadron absorber of a given muon identifier. The three muon identifiers, μ_1, μ_1' and μ_2, serve to test the internal consistency of our treatment of the data. The largest solid angle is achieved with μ_1, but for μ_1' the measured values of ϵ_p are smaller than for μ_1, and for μ_2, which has the smallest solid angle, the value of ϵ_p is zero. Furthermore, the dependence of ϵ_{μ} on the spatial position of the event vertices and on the energy of the hadron cascades of the $\nu_{\mu}(\bar{\nu}_{\mu})$-induced events is significantly different for the three muon identifiers. The values of the muon detection efficiencies given in Table I are based on directly measured muon angular distributions using muon identifier μ_1' for each of the data samples.[4] Included also in Table I are the numbers of events in each sample, the values of the mixing parameter α, and the corrected ratios R. The mean total energy of the events observed is about 45 GeV for the horn beam and about 53 GeV for the sign-selected beams.

Observe that the two subsets of the mixed beam data (rows 1 and 2) have appreciably different admixtures of ν and $\bar{\nu}$, as indicated by the different values of α, and that the data for the sign selected beams (rows 3 and 4), with very small and very large values of α, yield R^{ν} and $R^{\bar{\nu}}$ almost directly and separately.

The maximum likelihood fit to the four data sets yields $R^{\nu} = 0.12_4 \pm 0.04$ and $R^{\bar{\nu}} = 0.32_7 \pm 0.08$, where the errors are statistical only. These values include interactions of a small number of electron-neutrinos (ν_e) in the incident beams. Electromagnetic showers arising from events with electrons in the final states produced by $\nu_e(\bar{\nu}_e)$ interactions are not readily distinguished in our detector from hadronic showers induced by $\nu_\mu(\bar{\nu}_\mu)$. Estimates of the ratio $\sigma(\nu_e + \text{nucleon} \to e^- + \text{hadrons})/\sigma(\nu_\mu + \text{nucleon} \to \mu^- + \text{hadrons})$ and of the same ratio for $\bar{\nu}_e$ and $\bar{\nu}_\mu$ are 1.7% and 0.5%, respectively. Subtracting these contributions, and folding in an additional uncertainty (arising primarily from the determination of the muon detection efficiency) of 0.03 in R^{ν} and 0.04 in $R^{\bar{\nu}}$, we obtain finally

$$R^{\nu} = 0.11 \pm 0.05$$

and

$$R^{\bar{\nu}} = 0.32 \pm 0.09$$

These results are plotted in Fig. 2 as are also the separate fits to the data taken with the sign-selected beams and the admixed beam. Results from the CERN Gargamelle experiment[5] at much lower energy are also included in Fig. 2.

It is clear from Fig. 2 that $R^{\bar{\nu}}$ is larger than R^{ν}. This may perhaps reflect the experimentally determined fact that the charged weak current cross section for neutrinos σ_c^{ν} is about 3 times larger than the corresponding cross section $\sigma_c^{\bar{\nu}}$ for antineutrinos in the energy region of these experiments,[6,7] presumably due to a parity violating V-A interference term. If then, for example, the effective neutral weak current cross sections σ_N^{ν} and $\sigma_N^{\bar{\nu}}$ that give rise to muonless events are equal, one would expect $R^{\bar{\nu}} \approx 3R^{\nu}$.

The locus of the last equation is the line starting at the origin in Fig. 2, which is seen to be consistent with the results of this experiment. Equality of σ_N^{ν} and $\sigma_N^{\bar{\nu}}$ would imply the absence of a V-A interference term in those cross sections, and, presumably, the absence of parity violation in those processes as well.[8]

In Fig. 2 we show in addition a prediction based on the Weinberg-Salam gauge model[9] of the weak interactions, in which neutral weak currents make a natural appearance. The extension to semileptonic processes has been made by various authors[10], who obtain the lower bound curve in Fig. 2. Our data are about 2 standard deviations away from that theoretical limit. Within experimental error, other interpretations of the numerical value of $R^{\bar{\nu}}/R^{\nu}$ are also possible.[11] Note that R^{ν} and $R^{\bar{\nu}}$ may depend on energy, either continuously or discontinuously through some threshold effect, which temporarily, at least, also contributes to the difficulty of delineating the matrix element of the effective neutral weak current.

It is a pleasure to acknowledge the aid and encouragement of the National Accelerator Laboratory staff. We thank D. Cheng and R. L. Piccioni for their early contributions to this work.

Table I. Summary of data for the four neutrino beam configurations.

Data Sample		Number of events	Muon Detection Efficiency*			α	R
			μ_1	μ_1'	μ_2		
Mixed Beam	Horn Off	255	.86	.77	.74	0.74 ± 0.06	0.18 ± 0.05
	Horn On	283	.89	.81	.80	0.45 ± 0.06	0.22 ± 0.05
Sign-selected $(\pi,K)^-$		100	.93	.87	.83	0.12 ± 0.05	0.34 ± 0.12
Sign-Selected $(\pi,K)^+$		188	.93	.87	.83	0.98 ± 0.01	0.13 ± 0.06

*The 3 muon identifiers μ_1, μ_1' and μ_2 are defined in reference 2.

Footnotes and References

* Supported in part by the U. S. Atomic Energy Commission

⊥ On leave of absence from Laboratoire de L'Accelerateur Lineaire, Orsay, France.

** Alfred P. Sloan Foundation Fellow, now at the University of Chicago, Chicago, Illinois 60637.

1. A. Benvenuti et al., Phys. Rev. Letters 32, 800 (1974).

2. B. Aubert, et al., Harvard-Pennsylvania-Wisconsin-NAL preprint, March, 1974; to be published in Phys. Rev. Letters.

3. See P. Limon, et al., NAL-Pub-73/66-EXP, to be published in Nucl. Instr. and Methods. During most of the data-taking hadrons having a mean energy of 140 GeV were selected, which resulted in a neutrino energy spectrum with a mean energy of 53 GeV and a spread of ± 20 GeV.

4. To take into account very large angle muons it is necessary to make a small correction to the angular distribution data to obtain the detection efficiencies given in Table I. This correction depends on the form of the distribution in the scaling variable $y = E_h/E_\nu$ for events with muons. For antineutrinos the y-distribution is not yet definitively determined by our data, but preliminary results suggest that at higher energies the anti-neutrino distribution is similar to that for neutrinos. Accordingly, we have used the same correction for neutrinos and antineutrinos in conjunction with the measured angular distributions to find the detection efficiencies in the last two rows of Table I. The effect is less than the error assigned to the detection efficiencies in computing the final values of R^ν and $R^{\bar{\nu}}$ and their errors.

5. F. J. Hasert et al., Phys. Letters, 46B, 138 (1973), and CERN preprint TC-L/Int. 74-1, to be published in Nuclear Physics B.

6. D. H. Perkins, Proc. of the XVI International Conference on High Energy Physics, Chicago-Batavia 4, 189 (1972); T. Eichten et al, Physics Letters B46, 274 (1973); B46, 281 (1973).

7. A. Benvenuti et al, Phys. Rev. Letters 30, 1084 (1973); 32, 125 (1974).

8. Suggestions to this effect have been made, for example, by: M. A. B. Bég and A. Zee, Phys. Rev. Letters 30, 675 (1973); J. J. Sakurai, Phys. Rev. D9, 250 (1974); H. Cheng and C. Y. Lo, M. I. T. preprint.

9. S. Weinberg, Phys. Rev. Letters 19, 1264 (1967). A. Salam, in: Elementary Particle Theory, ed. N. Svartholm (Almquist and Forlag, Stockholm, 1968).

10. A. Pais and S. B. Treiman, Phys. Rev. D6, 2700 (1972). E. A. Paschos and L. Wolfenstein, Phys. Rev. D7, 91 (1973). L. M. Sehgal, Nuclear Physics B65, 141 (1973). C. H. Albright, Phys. Rev. D8, 3162 (1973).

11. For reviews and extensive references, see E. S. Abers and B. W. Lee, Phys. Reports 9C, No. 1 (1973), and M. A. B. Bég and A. Sirlin, to be published. Also A. Pais and S. B. Treiman, Preprint COO-2232B-33 (1973).

Figure Captions

Fig. 1. (a) Distribution of event occurrence times with respect to the start of the master gate. (b) Variation of the neutrino-antineutrino admixture α with event occurrence time, which reflects the on-time of the magnetic horn.

Fig. 2. Results for R^{ν} and $R^{\bar{\nu}}$ from this experiment. The dotted cross represents results from the sign-selected beams; the dashed cross is from the mixed neutrino-antineutrino beam, for which R^{ν} and $R^{\bar{\nu}}$ are strongly correlated, as indicated by the orientation of the error bars. The solid circle with its error bars shows the result of a fit to all the data, including systematic errors. All three points are the results after subtraction of the ν_e contribution. The open circle point is from reference 5. The curve marked THEORY LIMIT is obtained from reference 11.

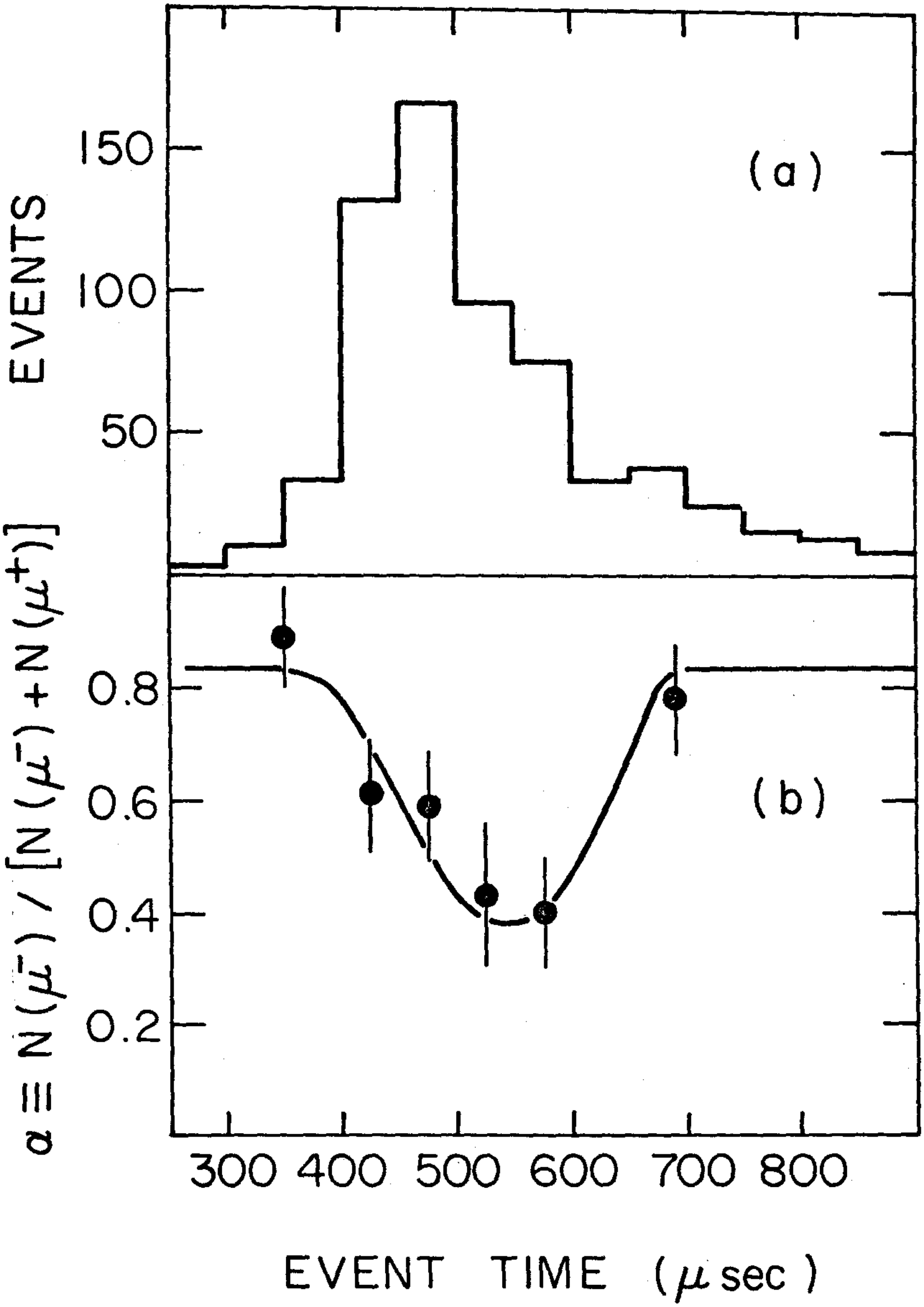

EVENTS
150
100
50
(a)
$a \equiv N(\mu^-) / [N(\mu^-) + N(\mu^+)]$
0.8
0.6
0.4
0.2
(b)
300 400 500 600 700 800
EVENT TIME (μ sec)

Fig. 1

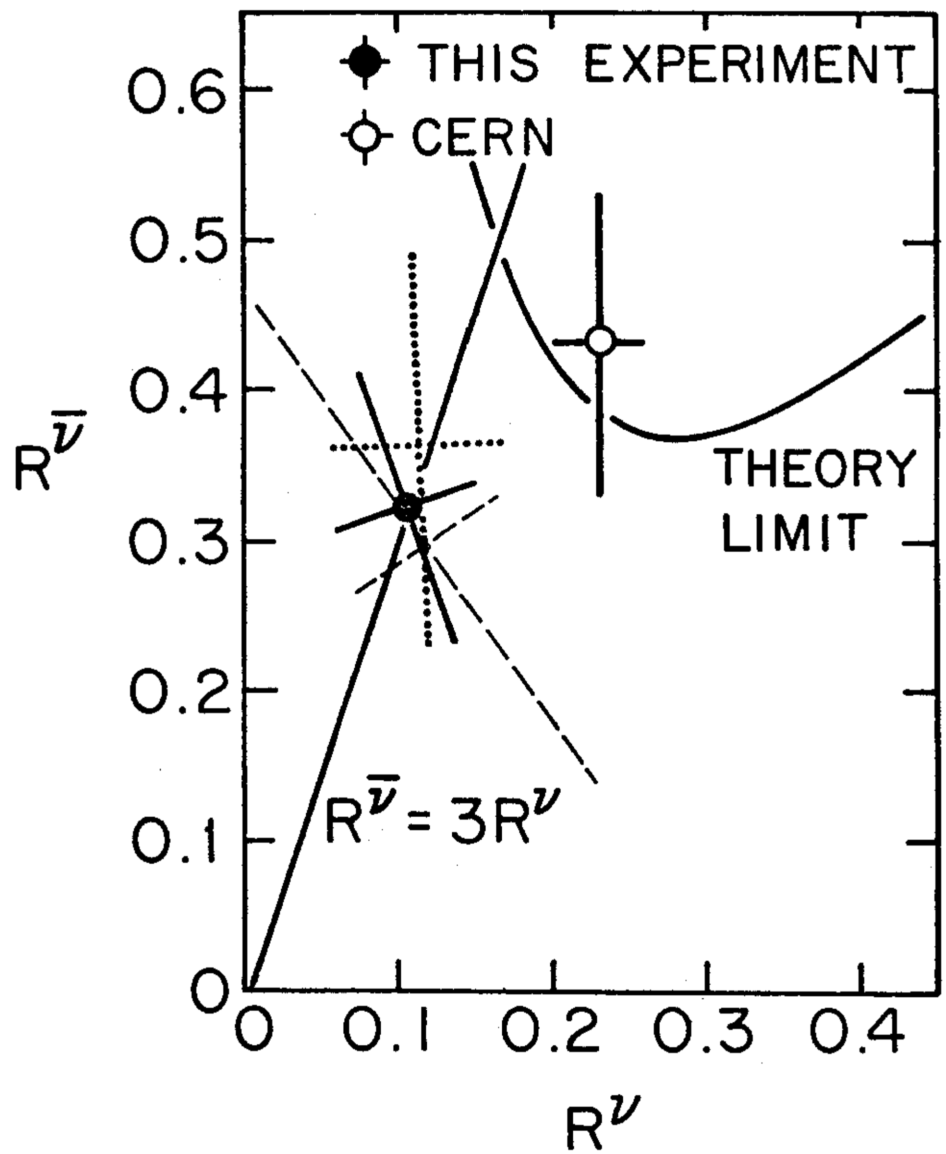
THIS EXPERIMENT
CERN
THEORY
LIMIT
$R^{\bar{\nu}} = 3R^{\nu}$
0.6
0.5
0.4
0.3
0.2
0.1
0
0
0.1
0.2
0.3
0.4
$R^{\bar{\nu}}$
R^{ν}

Fig. 2